Int. J. Solids Structures, 1967, Vol. 3, pp. 309 to 332. Pergamon Press Ltd. Printed in Great Britain

NUMERICAL BIHARMONIC ANALYSIS AND SOME APPLICATIONS

M. A. JASWON and M. MAITI
Institute of Theoretical and Applied Mechanics, University of Kentucky, Kentucky

and

G. T. SYMM
Mathematics Division, N.P.L., Teddington, England

Abstract—It is shown that biharmonic boundary value problems can be formulated in terms of integral equations. Procedures are given for solving such equations numerically, for smoothing out sharp corners on the boundary, and for checking results. These techniques are applied to attack some two-dimensional stress problems which do not seem to be amenable to any other treatment.

INTRODUCTION

A FORMULATION has been given of two-dimensional linear elastostatics in terms of boundary integral equations [1]. These equations do not submit to any readily accessible analytical treatment, and they also provide difficulties for a numerical treatment owing to the presence of singular kernels. Considerable progress has, however, recently been made with the numerical solution of various singular integral equations appertaining to potential theory [2,3]. These are closely related to the elastostatic integral equations, thereby opening the way to an effective numerical attack upon the latter. In this paper we present a modernized version of the original formulation and extend it to exterior domains, and we apply the theory to solve some problems of engineering interest that do not seem to have been solved by any other method. These problems fall into two main classes. First, we consider bars containing V-shaped and semi-circular notches subject to uniform applied tension or bending, the results being plotted as contours of constant maximum shear stress and of constant hydrostatic pressure. Substantial agreement is found with the results of Southwell and Allen [4] for the only problems of this class which they seem to have attacked, i.e. uniform applied tension. The second class of problem, drawn from the field of soil mechanics, concerns an infinite medium subject to tractions along an internal boundary. All these problems are equilibrated traction problems. Displacement problems, mixed problems, non-equilibrated traction problems, problems of ring-shaped domains, and transverse loading of thin plates, may be covered by suitable adaptions of the formulation. These will be treated in subsequent papers. Eventually, therefore, most two-dimensional problems of engineering interest should be brought within the scope of a common integral equation approach.

The whole process of formulating a boundary integral equation, replacing it by a discrete linear system corresponding to a set of nodal points spaced along the boundary, handling the singular kernel, solving this system, and utilizing the solution to generate the

stress function and stress components over any selected region, can be effected by a single digital computer program. This feature enables two independent checks on the solution to be made with hardly any further human effort. First, we start with a relatively small number, n, of nodal points and examine how the numerical solution behaves as n increases: ill-conditioned behavior would indicate an inadequate numerical approximation at one or more stages, or possibly a breakdown in the formulation. Secondly, we can always introduce an arbitrary known stress function into any given domain, compute its boundary values and boundary normal derivatives, and use these to generate interior values of the function or of its derivatives for comparison with those initially introduced: since this test problem differs only trivially from the actual one as regards its numerical solution, it should reveal at once any straightforward sources of error. These two types of check are always incorporated into our procedures.

Our approach to mathematical elastostatics contrasts with Muskhelishvili's well known complex variable approach [5], which requires the domain under consideration to be mapped into the unit circle or half-plane. A ring-shaped domain must be mapped into the region between two concentric circles. Closed expressions for the mapping function exist for relatively few compact domains, and for hardly any ring-shaped domains. Approximate expressions for the mapping function may sometimes be constructed by integral equation methods [6]. However, even after this step has been completed, several further steps must be undertaken before the stress field can actually be computed. It is difficult to believe, and it has not to our knowledge ever been demonstrated, that this sequence of steps could be as efficient as that outlined above. Other approaches, such as the hypercircle method of Synge and Prager [7], the kernel function method of Bergman and Shiffer [8], the point-matching technique of Niedenfuhr and Hulbert [9], and the relaxation technique of Southwell and Allen [10], are each effective for specialized types of problems, but are not sufficiently general to cope with the variety of domains and boundary conditions that arise in modern engineering science.

The rest of the text divides into three main sections: biharmonic analysis; some trial problems to clarify our numerical techniques; and some selected problems of interest which fall within the scope of the theory presented.

BIHARMONIC ANALYSIS

A function χ which is continuous, and has continuous derivatives up to the fourth order throughout a finite compact domain D, and which satisfies the biharmonic equation $\nabla^2(\nabla^2\chi) = 0$ in D, is uniquely determined within D if χ, χ' (inward normal derivative) are prescribed on the boundary L of D. We may adopt throughout D the representation

$$\chi = r^2\phi + \psi; \qquad \nabla^2\phi = \nabla^2\psi = 0 \tag{1}$$

where $r^2 = x^2 + y^2$, or equivalent representations such as $x\phi + \psi$ or $y\phi + \psi$ depending on convenience. As shown in Appendix I, the former representation has a uniqueness not shared by the latter two, so rendering it superior from the viewpoint of numerical analysis. Since χ is prescribed on L, equation (1) may be viewed as a linear functional relation coupling ϕ, ψ on L. Also, since χ' is prescribed on L, there exists a linear functional relation

$$\chi' = (r^2\phi)' + \psi' = 2rr'\phi + r^2\phi' + \psi' \tag{2}$$

coupling the normal derivatives ϕ', ψ' on L. It is possible in principle to determine the four boundary functionals ϕ, ψ, ϕ', ψ'—and to determine them uniquely—from χ, χ' on L. Thus, the existence theorem ensures that we can construct a unique χ throughout D from χ, χ' on L; hence we may compute the harmonic function

$$\nabla^2\chi = 4\left(x\frac{\partial\phi}{\partial x}+y\frac{\partial\phi}{\partial y}+\phi\right) \tag{3}$$

throughout $D+L$ and hence* also ϕ throughout $D+L$; hence a unique ψ can be computed throughout $D+L$, and therefore a unique ϕ, ψ, ϕ', ψ' can be computed along L. One specific construction procedure, suggested by Jaswon [1], is to introduce Green's boundary formula

$$[h, h'] - \pi h = 0 \tag{4}$$

connecting any harmonic function h with its normal derivative h' along L. Putting $h = \phi$ and ψ in turn, and coupling (4) with (1) and (2), yields a system of four linear functional equations capable of yielding the four boundary quantities required. This system effectively reduces to two on noting that

$$[\chi, \chi'] - \pi\chi = [r^2\phi, (r^2\phi)'] - \pi r^2\phi \tag{5}$$

and coupling (5) with (4) where $h = \phi$.

Although the preceding reduction has been proved to work well [3], it suffers from two limitations. First, it yields directly only the boundary quantities, which must then be continued into D either by Green's formula or by some other means. Secondly, it is not well adapted towards computing the second derivatives of χ, which provide the stress components. A more efficient alternative to (4) is obtained by identifying ϕ, ψ as potentials generated by continuous simple source distributions on L, with densities to be determined. Thus we write

$$\phi(\mathbf{P}) = \int \log|\mathbf{P}-\mathbf{q}|\sigma(\mathbf{q})\,\mathrm{d}q \tag{6}$$

where $\mathbf{q}$ is a vector variable defining points on L, $\mathrm{d}q$ denotes the arc differential at $\mathbf{q}$ directed so as to keep D on the left, $\sigma(\mathbf{q})$ is the source density at $\mathbf{q}$ to be determined, and $\mathbf{F}$ is a vector variable defining points within D. This potential remains continuous as $\mathbf{P}$ approaches any point $\mathbf{p}$ of L, and so on L we may write

$$\phi(\mathbf{p}) = \int \log|\mathbf{p}-\mathbf{q}|\sigma(\mathbf{q})\,\mathrm{d}q \tag{7}$$

where $\phi(\mathbf{P}) \to \phi(\mathbf{p})$ as $\mathbf{P} \to \mathbf{p}$. It is a known result [11] that

$$\phi'(\mathbf{p}) = \int \log'|\mathbf{p}-\mathbf{q}|\sigma(\mathbf{q})\,\mathrm{d}q + \pi\sigma(\mathbf{p}) \tag{8}$$

where $\log'|\mathbf{p}-\mathbf{q}|$ signifies the inward normal derivative of $\log|\mathbf{p}-\mathbf{q}|$ at $\mathbf{p}$ keeping $\mathbf{q}$ fixed, and it follows automatically from (8) that $\int\phi'(\mathbf{p})\,\mathrm{d}p = 0$ as expected. Given ϕ on L, (7) becomes a Fredholm singular integral equation of the first kind for σ. Apart from certain exceptional boundaries discussed by Jaswon [1], σ may be uniquely determined. Similarly, given ϕ' on L satisfying $\int\phi'(\mathbf{p})\,\mathrm{d}p = 0$, (8) becomes a Fredholm integral equation of the

* Writing $\nabla^2\chi = \sum C_nS_n$, where S_n is a plane harmonic function of degree n, it can be seen that

$$\phi = \tfrac{1}{4}\sum\frac{C_nS_n}{(n+1)}$$

second kind for σ. Successful techniques for the numerical solution of (7) and (8) have been developed by Symm [2, 3] and by Maiti [12], extending preliminary work by Jaswon and Ponter [13]. These are briefly outlined in Appendix II. Writing

$$\psi(\mathbf{p}) = \int \log|\mathbf{p}-\mathbf{q}|\mu(\mathbf{q})\,dq, \qquad \psi'(\mathbf{p}) = \int \log'|\mathbf{p}-\mathbf{q}|\mu(\mathbf{q})\,dq + \pi\mu(\mathbf{p}) \tag{9}$$

where $\mu(\mathbf{q})$ is a source density at $\mathbf{q}$ to be determined, and substituting from (7), (8), (9) into (1) and (2), we arrive at two coupled linear integral equations for σ and μ. This coupled system is not of the Fredholm type, but has a simple structure and exhibits a unique solution, i.e. that which would be obtained by solving directly for ϕ, ψ on L as described above and then solving for σ, μ from (7), (9) respectively. With these known, the harmonic functions ϕ and ψ, and hence also χ, can be generated at any point $\mathbf{P}$ of D. So far as we are aware, this formulation of biharmonic boundary value problems is not very well known and has not previously been exploited.

Derivatives of χ can be found either by numerical differentiation or by utilizing differentiated kernels. Thus, for instance

$$\chi_{xx} = 2\phi + r^2\phi_{xx} + 4x\phi_x + \psi_{xx} \tag{10}$$

where

$$\phi_x(\mathbf{P}) = \int \log_x|\mathbf{P}-\mathbf{q}|\sigma(\mathbf{q})\,dq, \text{ etc.}$$

In particular, as follows from (3), the hydrostatic pressure $\nabla^2\chi$ may be computed to a higher accuracy than the individual stress components. Generally speaking, formulae such as (10) work well except near L itself, at which region it is preferable to utilize numerical differentiation of χ.

In traction problems of two-dimensional elasticity, the boundary partial derivatives of χ at $\mathbf{p}$ are evaluated from

$$\frac{\partial\chi}{\partial x} \equiv \chi_x = -\int^{\mathbf{p}} F_y\,dq + \alpha, \qquad \frac{\partial\chi}{\partial y} \equiv \chi_y = \int^{\mathbf{p}} F_x\,dq + \beta \tag{11}$$

where F_x, F_y are the traction components per unit length at $\mathbf{q}$, and α and β are arbitrary constants of integration relative to some arbitrary origin of integration on L. These partial derivatives yield the canonical boundary quantities

$$\begin{aligned} \chi' &= \chi_x x' + \chi_y y' \\ \chi &= \gamma + \int(\chi_x\,dx + \chi_y\,dy) \end{aligned} \tag{12}$$

where γ is a further constant of integration. Note that χ' includes a term $\alpha x' + \beta y'$ and χ includes a corresponding term $\alpha x + \beta y + \gamma$: these are respectively the boundary normal derivatives and boundary values of a harmonic function $\alpha x + \beta y + \gamma$ existing in D, which makes no contribution to the stresses. As a corollary, neither the location of the origin of integration, nor the values there of χ_x, χ_y, χ can have any physical significance. It may be readily proved that χ must be a single-valued function for a compact domain subject to equilibrated boundary tractions.

Given an infinite domain D_e external to some closed curve L, suitably restricted harmonic functions may be represented throughout D_e by simple source potentials of the form $\int\log|\mathbf{P}-\mathbf{q}|\sigma(\mathbf{q})\,dq$ where dq stands for the arc differential at $\mathbf{q}$ directed so as to keep

D_e on the left. It is a straightforward but nontrivial fact that

$$\int \log|\mathbf{P}-\mathbf{q}|\sigma(\mathbf{q})\,dq \to \log r \int \sigma(\mathbf{q})\,dq + O(1/r) \tag{13}$$

as $r \equiv |\mathbf{P}| \to \infty$. The absence of a constant on the right-hand side of (13) shows that no constant harmonic function may be represented in D_e by a simple source potential (though it could within D_i). Neither can the harmonic functions x or y in D_e be so represented, since they behave as $O(r)$ at infinity. Accordingly, since

$$\chi \to \alpha x + \beta y + O(\log r) \quad \text{as} \quad r \to \infty \tag{14}$$

in the absence of finite stresses at infinity and in the absence of dislocations [14], the representation (1) evidently requires some modification. This is achieved by writing

$$\chi = r^2\phi + \psi + \gamma \tag{15}$$

where γ is a constant to be determined, where

$$\psi \equiv \psi(\mathbf{P}) = \int \log|\mathbf{P}-\mathbf{q}|\mu(\mathbf{q})\,dq, \tag{16}$$

and where

$$\phi \equiv \phi(\mathbf{P}) = \int \log|\mathbf{P}-\mathbf{q}|\sigma(\mathbf{q})\,dq, \tag{17}$$

subject to the condition

$$\int \phi'(\mathbf{q})\,dq = 2\pi \int \sigma(\mathbf{q})\,dq = 0. \tag{18}$$

Condition (18) ensures that $\phi = O(1/r)$ as $r \to \infty$, so eliminating the possibility

$$r^2\phi \to O(r^2 \log r) \quad \text{as} \quad r \to \infty$$

which implies the presence of a radial fissure [14] (i.e. a two-dimensional dislocation singularity yielding a multi-valued local rotation on circuiting the origin). No such restriction applies to ψ. To see that (15) can embrace the terms $\alpha x + \beta y$ of (14), we put

$$\phi = \alpha\frac{\cos\theta}{r} + \beta\frac{\sin\theta}{r}, \qquad \psi = 0, \qquad \gamma = 0$$

and note that

$$r^2\left(\alpha\frac{\cos\theta}{r} + \beta\frac{\sin\theta}{r}\right) = \alpha r\cos\theta + \beta r\sin\theta = \alpha x + \beta y.$$

Since χ is assigned on L, (15) may be viewed as a linear functional relation between ϕ, ψ and γ on L. Also, since χ' is assigned on L, we obtain a linear functional relation

$$\chi' = (r^2\phi)' + \psi' = 2rr'\phi + r^2\phi' + \psi' \tag{19}$$

between ϕ, ϕ' and ψ' on L, the positive unit normal being directed into D_e. These relations, together with (18), suffice to determine σ, μ and γ and hence ϕ, ψ throughout D_e by virtue of (16), (17) and hence χ throughout D_e by virtue of (15). This χ is unique, since it behaves according to (14) at infinity and satisfies the requisite boundary conditions on L. The uniqueness of ϕ, ψ is examined in Appendix I. It has been assumed that the tractions on L form a self-equilibrated system. If not, we merely supplement the representation (15) by introducing functions corresponding to the asymptotic behavior of the resultant force and couple

on L. Semi-infinite problems are not covered directly by our formulation. They can be adapted, however, by reflecting the problem into a suitable imagined mirror and closing the boundary. Although the symmetrized stress field necessarily exhibits a different asymptotic behavior from the original, these two fields do not differ significantly at the region of interest which neighbors the boundary.

SOME TRIAL PROBLEMS

The simplest possible trial function one can envisage is

$$\chi = r^2 \equiv r^2 \,.\, 1 + 0 \tag{20}$$

where $\phi = 1, \psi = 0$. This means that σ and μ satisfying (1), (2) for $\chi = r^2$, $\chi' = 2rr'$ may be identified as the solutions of

$$\int \log|\mathbf{p}-\mathbf{q}|\sigma^*(\mathbf{q})\,dq = 1, \qquad \int \log|\mathbf{p}-\mathbf{q}|\mu^*(\mathbf{q})\,dq = 0 \tag{21}$$

for the boundary L in question. Apart from the exceptional boundaries discussed by Jaswon [1], it follows from (21) that $\mu^* = 0$. Also, σ^* can be calculated to a high accuracy without any difficulty. Let us now compare the numerical values of σ, μ with σ^*, μ^* respectively, for the ellipse defined by

$$x^2/a^2 + y^2/b^2 = 1; \qquad a = 2, \qquad b = 1. \tag{22}$$

It is evident that all the quadrants of the ellipse are equivalent, so that the effective number of unknowns reduces from n to $n/4$. We divide L into equal intervals using elliptic integrals, and choose $n = 8$ initially as shown in Fig. 1(a). The nodal values of σ^* for $n = 32$, calculated numerically from (21), are displayed in the third column of Table 1, it being understood that

$$\begin{aligned} \sigma_1^* &= \sigma_{16}^* = \sigma_{17}^* = \sigma_{32}^* \\ \sigma_2^* &= \sigma_{15}^* = \sigma_{18}^* = \sigma_{31}^*, \text{ etc.} \end{aligned} \tag{23}$$

TABLE 1. ELLIPSE: ANALYTICAL AND NUMERICAL NODAL VALUES OF σ^*, σ, μ FOR $n = 32$, $\chi = r^2$

i	Analytical σ_i^*	Numerical σ_i^*	σ_i	μ_i
1	0·38003	0·38183	0·37585	0·02225
2	0·32054	0·32050	0·32624	−0·02918
3	0·27141	0·27101	0·27177	−0·00220
4	0·24000	0·23968	0·23981	−0·00015
5	0·22011	0·21988	0·21981	−0·00024
6	0·20758	0·20738	0·20733	0·00013
7	0·20015	0·20018	0·19981	0·00038
8	0·19668	0·19664	0·19660	−0·00003

The corresponding analytically determined values appear in the second column. The corresponding nodal values of σ and μ, calculated numerically from (1), (2), appear in the fourth and fifth columns respectively. It will be seen that σ agrees to within 2 per cent with both the analytical and numerical σ^* and that $\mu = O(10^{-2})$, which is a good numerical counterpart to the analytical solution $\mu^* = 0$.

We now consider (20) as appertaining to the square defined by

$$x = \pm a, \qquad y = \pm a, \qquad a = 1/2 \tag{24}$$

choosing $n = 16$ initially as shown in Fig. 1(b). The numerical nodal values of σ^* are displayed in Table 2 for $n = 64$, it being noted that

$$\sigma_1^* = \sigma_{16}^* = \sigma_{17}^* = \sigma_{32}^* = \sigma_{33}^* = \sigma_{48}^* = \sigma_{49}^* = \sigma_{64}^*, \text{etc.}, \tag{25}$$

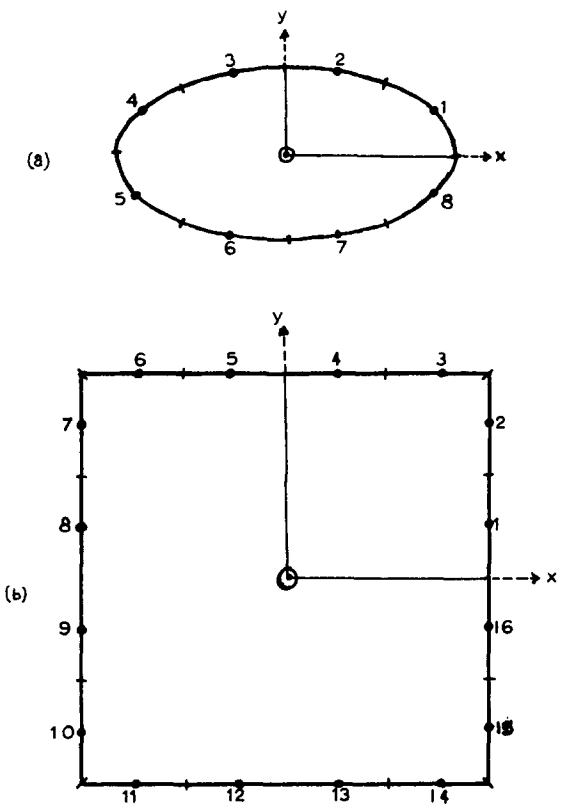

FIG. 1. Initial subdivision of ellipse and square.

TABLE 2. SQUARE: NODAL VALUES OF σ^* FOR $n = 64$, $\chi = r^2$

i	σ_i^*
1	−0·36188
2	−0·36607
3	−0·37499
4	−0·39002
5	−0·41396
6	−0·45427
7	−0·51399
8	−0·90447

by virtue of symmetry. No analytically determined values seem to be available for comparison. When an attempt is made to solve (1), (2) numerically for σ and μ, ill-conditioning now appears as indicated by the strongly fluctuating values displayed in Table 3 for $n = 32$. This trouble arises essentially from the fact that the expressions (8), (9) for ϕ', ψ' behave badly from the numerical standpoint near a corner. Fortunately, however, the trouble

TABLE 3. SQUARE: NODAL VALUES OF σ, μ FOR $n = 32$, $\chi = r^2$

i	σ_i	μ_i
1	−0·38621	0·00693
2	−0·23792	−0·04498
3	−0·84816	0·16374
4	−0·35387	−0·15173

can to a large extent be eliminated by "rounding off" the corner as follows: replace the two intervals (each of length h) adjoining the corner by a quadrant of an inscribed circle of radius h, divide the quadrant into two arcs each of length $\pi h/4$, and introduce a nodal point into the middle of each to replace the original two. Accordingly, as exhibited in Fig. 2, we approximate steadily to the corner by a sequence of circular quadrants of decreasing radius as n increases. The ratio of the curved interval to the straight line interval remains constant at $\pi/4:1$, and the curvature increases as $1/h$. Squares with rounded off corners will henceforth be termed "pseudo-squares". Numerical nodal values of σ and μ for the pseudo-square appear in Table 4, these being of course subject to the symmetry (25). They are seen to be reasonably well conditioned, and $\mu = O(10^{-2})$ as expected; also, σ agrees tolerably well with σ^* recalculated for the pseudo-square, which in turn agrees well with σ^* of Table 2 for the actual square.

As a first trial problem for exterior domains, we consider an infinite medium containing an elliptic internal boundary, e.g. defined by (22), subject to a uniform normal pressure P. This implies that

$$F_x = P\frac{dx}{dn} = -P\frac{dy}{ds}. \qquad F_y = P\frac{dy}{dn} = P\frac{dx}{ds}$$

whence

$$\begin{aligned} \chi_x &= -Px, \qquad \chi_y = -Py \\ \chi' &= -P(xx'+yy'), \qquad \chi = -P(x^2+y^2)/2 \end{aligned} \tag{26}$$

along L, on choosing the constants of integration to produce the maximum possible symmetry. To effect a numerical solution of (15), (18) and (19) for the boundary quantities (26), we choose successively $n = 16, 32, 64$ bearing in mind that the effective number of unknowns reduce to $n/2+1$ owing to symmetry. A well known analytic solution is available for comparison [3].

The maximum shear stress and hydrostatic pressure are given by

$$\begin{aligned} S &= \{(p_{xx}-p_{yy})^2+4p_{xy}{}^2\}^{\frac{1}{2}}/2 \\ H &= p_{xx}+p_{yy} \end{aligned} \tag{27}$$

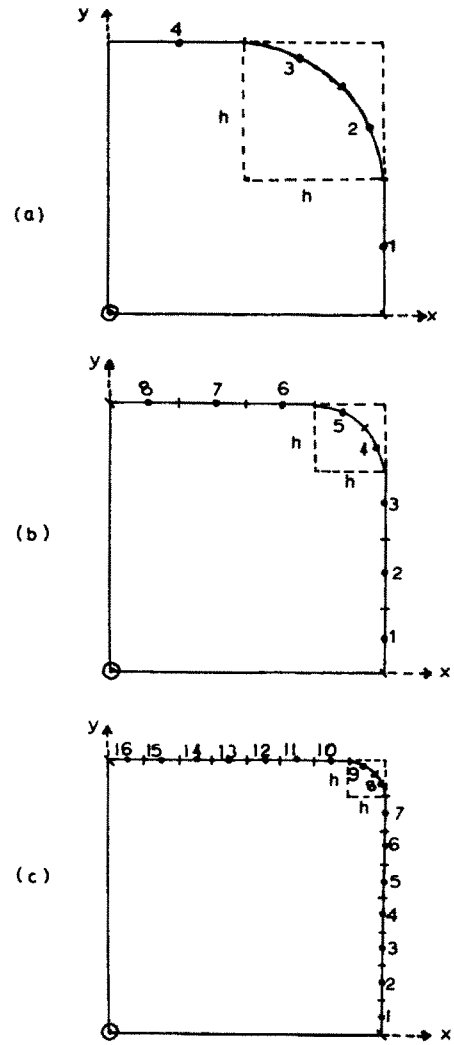

FIG. 2. A sequence of pseudo-squares converging to a square of which only one-quarter is shown in the Figures.

TABLE 4. PSEUDO-SQUARE: NODAL VALUES OF σ^*, σ, μ FOR $n = 64$, $\chi = r^2$

i	σ_i^*	σ_i	μ_i
1	−0·36285	−0·36910	−0·00014
2	−0·36680	−0·36641	−0·00013
3	−0·37638	−0·37504	−0·00041
4	−0·39270	−0·39355	0·00022
5	−0·41949	−0·41034	−0·00324
6	−0·46481	−0·47885	0·00490
7	−0·57808	−0·61825	0·01814
8	−0·97929	−0·92025	−0·02639

respectively. Numerically determined values of S for $n = 64$, compared with their numerical counterparts, are exhibited in Fig. 3.

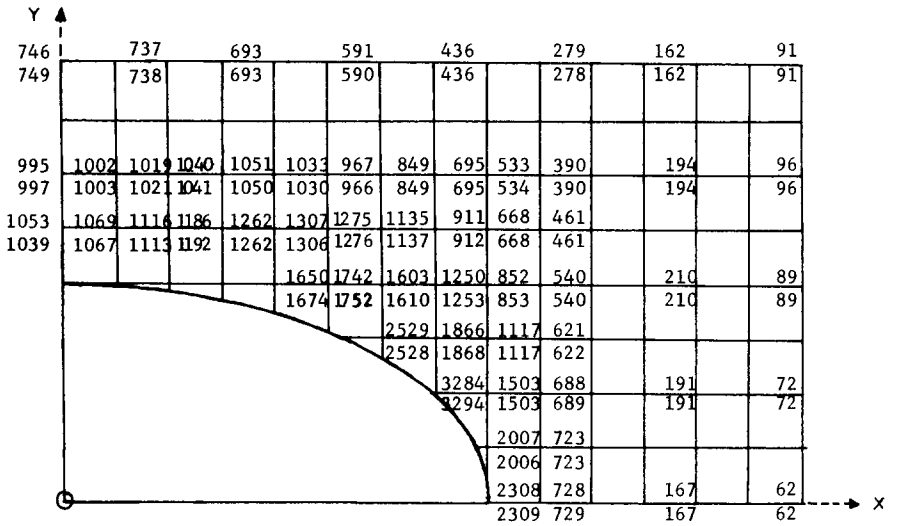

FIG. 3. Generated values of 4000 S^2 (lower) compared with its analytic values (upper) around elliptic cavity.

A second, more difficult, trial problem, is the semi-infinite medium subject to a uniform pressure P distributed over a finite interval $-a \leq x \leq a$ of its plane boundary. The pressure distribution has the asymptotic effect of a concentrated force $2Pa$ located at $x = y = 0$, generating the well-known stress function

$$\chi_\infty = \frac{2Pa}{\pi} x\theta. \tag{28}$$

Since the harmonic function θ cannot be represented by a simple source potential, χ_∞ cannot be embraced by (15) and must therefore be eliminated at the outset. Mathematically speaking, if χ is the true solution, one attempts to calculate $\chi - \chi_\infty$ numerically rather than χ itself. An alternative, less exact but more manageable approach, is to reflect the problem into the x-axis and so convert the semi-infinite medium into an infinite medium subject to equilibrated tractions. If the domains $y > 0$, $y < 0$ are separated by a sufficiently long, though finite, cut, the stress pattern in the region of interest should differ but little from that of the semi-infinite problem. It is convenient in practice to make the cut of finite width [Fig. 4(a)], thereby avoiding extremely sharp angles at its extremities and rendering the preceding methods applicable. If the rectangular cavity in question is bounded by $x = \pm X$, $y = \pm d$ we have

$$F_x = 0 \text{ everywhere on } L,$$

$$F_y = \pm P \text{ along } |x| \leq a,\ y = \pm d \text{ respectively},$$

$$F_y = 0 \text{ elsewhere on } L.$$

Hence, from (11), remembering that $ds = \pm dx$ along $y = \pm d$ respectively,

$$\chi_y = 0 \text{ everywhere on } L,$$

$$\chi_x = -Px \text{ along } |x| \leq a,\ y = \pm d \text{ choosing } \chi_x = 0 \text{ when } x = 0,$$

$$= -Pa \text{ along } x \geq a,$$

$$= Pa \text{ along } x \leq -a.$$

Hence

$$\begin{aligned}
\chi' &= \chi_x x' \\
&= 0 \text{ along } y = \pm d \text{ since } x' = 0 \text{ along } y = \pm d, \\
&= -Pa \text{ along } x = +X \text{ since } x' = 1 \text{ along } x = +X, \qquad (29) \\
&= -Pa \text{ along } x = -X \text{ since } x' = -1 \text{ along } x = -X, \\
&= -Pa\,|x'| \text{ along } x = \pm X,
\end{aligned}$$

$$\begin{aligned}
\chi &= \int \chi_x \, dx \\
&= -P(x^2 + a^2)/2 \text{ along } |x| \leq a,\ y = \pm d \\
&= -Pax \text{ along } x \geq a, \qquad (30) \\
&= Pax \text{ along } x \leq -a, \\
&= -Pa\,|x| \text{ along } |x| \geq a,
\end{aligned}$$

bearing in mind continuity and choosing the constant of integration to produce the maximum possible symmetry.

On replacing the extremities of the cavity by semi-circles of radius d as indicated [Fig. 4(b)], the formulae (29), (30) still apply*. Taking $a = d = 2$, $X = 18$, this problem has been solved numerically for an initial subdivision $n = 64$ exhibited in Fig. 4(c), and also for $n = 128$. Table 5 compares the numerically determined S at some interior points for

TABLE 5. VALUES OF 4000 S^2 FOR THE DISTRIBUTED PRESSURE PROBLEM (Fig. 4)

y	x	Numerical		Analytic
		$n = 64$	$n = 128$	
1·2	0·0	327	327	316
	0·8	360	361	349
	1·6	408	414	405
	2·4	278	283	281
	3·2	108	114	114
2·0	0·0	419	411	405
	0·8	413	408	403
	1·6	372	371	368
	2·4	265	268	267
	3·2	151	153	154

* Replace $x = \pm X$ by $|x| \geq X$ in (29).

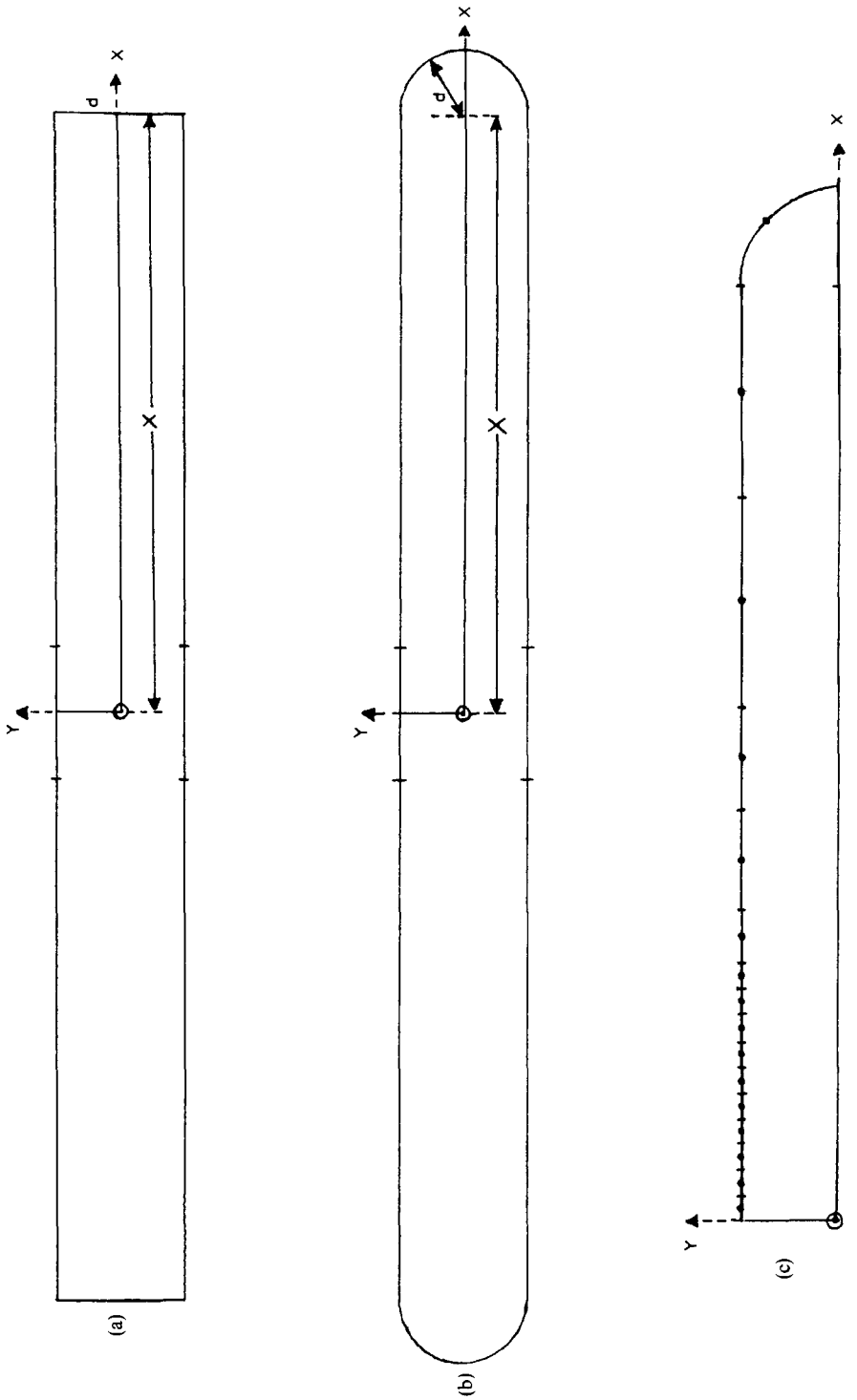

FIG. 4. Successive stages in smoothing and subdividing a cut of finite width.

these two subdivisions together with their analytical counterparts as calculated from the exact solution

$$\chi = \frac{P}{2\pi}(r_+^2\theta_+ - r_-^2\theta_-) - \frac{Pa}{\pi}y \tag{31}$$

of the original semi-infinite problem, where $r_\pm, \theta_\pm$ are polar co-ordinates centred about $\pm a, 0$ respectively. It will be seen that the numerical results are well conditioned, and provide reasonable accuracy in the region of interest. The contours of constant S do not differ significantly from those exhibited for the shallow trench in Fig. 14.

A further selection of trial problems may be found in [3] and [12].

NOTCHED BAR AND TRENCH PROBLEMS

We now consider the extensional problem for a rectangle of dimensions 2:1 containing two symmetrically situated semi-circular notches [Fig. 5(a)]. Because of symmetry, attention need be focused only on the quadrant ABCF. Fig. 5(b) exhibits the initial subdivision ($n = 56$), characterized by a constant interval length h on the straight boundary and with the corner B rounded off as before. The corner C is rounded off as shown. Fig. 5(c) exhibits the second subdivision, where a similar procedure has been applied.

The most appropriate test function for this problem is

$$\chi = y^2 = r^2 \cdot \tfrac{1}{2} + (y^2 - x^2)/2, \tag{32}$$

since it would be the solution if the notches were absent. On inserting $\chi = y^2, \chi' = 2yy'$ into (1), (2) and solving numerically for σ and μ, we generate the stress component $p_{xx} (= \chi_{yy})$ over those points indicated in Fig. 6(a). The component is seen to be constant everywhere, as expected, except very near L. Also, the numerical σ, μ compare well with σ^*, μ^* calculated numerically from

$$\int \log|\mathbf{p} - \mathbf{q}|\sigma^*(\mathbf{q})\,dq = \tfrac{1}{2}, \qquad \int \log|\mathbf{p} - \mathbf{q}|\mu^*(\mathbf{q})\,dq = (y^2 - x^2)/2. \tag{33}$$

These results show that our integral equation procedures may be applied with confidence to notched domains. As regards the actual problem, we have from (11) that

$$\begin{aligned}
&\chi_x = 0 \text{ everywhere on } L \text{ since } F_y = 0 \text{ everywhere on } L,\\
&\chi_y = y \text{ on AB taking } F_x = 1 \text{ on AB and choosing } \chi_y = 0 \text{ when } y = 0,\\
&\quad = \tfrac{1}{2} \text{ on BCF since } F_x = 0 \text{ on BCF, bearing in mind that } \chi_y \text{ remains continuous at B.}\\
&\chi' = \chi_x x' + \chi_y y' = \chi_y y'\\
&\quad = 0 \text{ on AB since } y' = 0 \text{ on AB,}\\
&\quad = -\tfrac{1}{2} \text{ on BC since } y' = -1 \text{ on BC,}\\
&\quad = y'/2 \text{ on the quadrant CF where } y' \text{ can be readily found.}
\end{aligned} \tag{34}$$

$$\begin{aligned}
&\chi = \int(\chi_x\,dx + \chi_y\,dy) = \int \chi_y\,dy\\
&\quad = y^2/2 \text{ on AB choosing } \chi = 0 \text{ when } y = 0,\\
&\quad = \tfrac{1}{2}(\tfrac{1}{2})^2 \text{ on BC since } dy = 0 \text{ on BC,}\\
&\quad = y/2 - \tfrac{1}{8} \text{ on the quadrant CF, bearing in mind that } \chi \text{ remains continuous at B and C.}
\end{aligned} \tag{35}$$

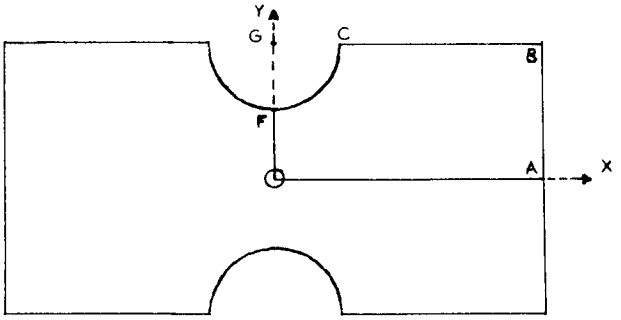

(a) Semi-circular notch of radius $\frac{1}{4}$.

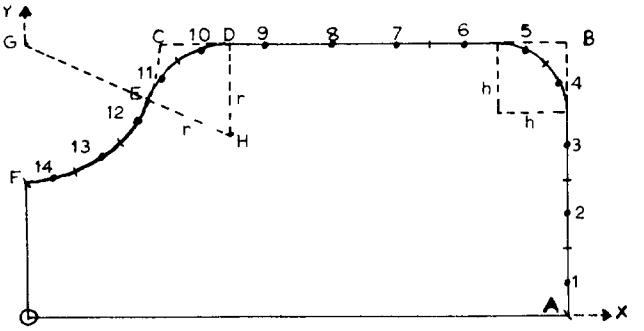

(b) Initial subdivision.

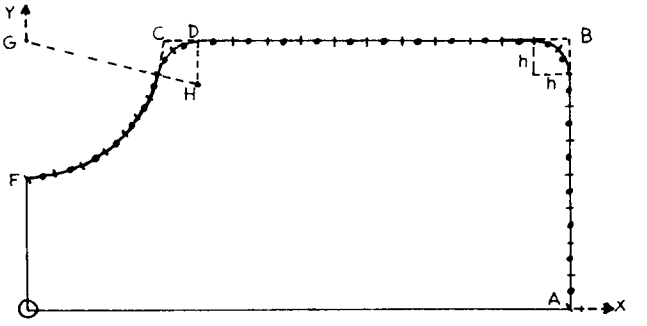

(c) Second and final subdivision.

FIG. 5. To round off the corner at C, we construct a circular arc tangential to BC at D (where DC is the last interval on BC) and tangential to the notch at E. If so, bearing in mind that GC = GE = $\frac{1}{4}$, we determine r by the equation

$$(\tfrac{1}{4}+r)^2 = r^2+(\tfrac{1}{4}+h)^2, \qquad \text{i.e.} \quad r = 2h^2+h.$$

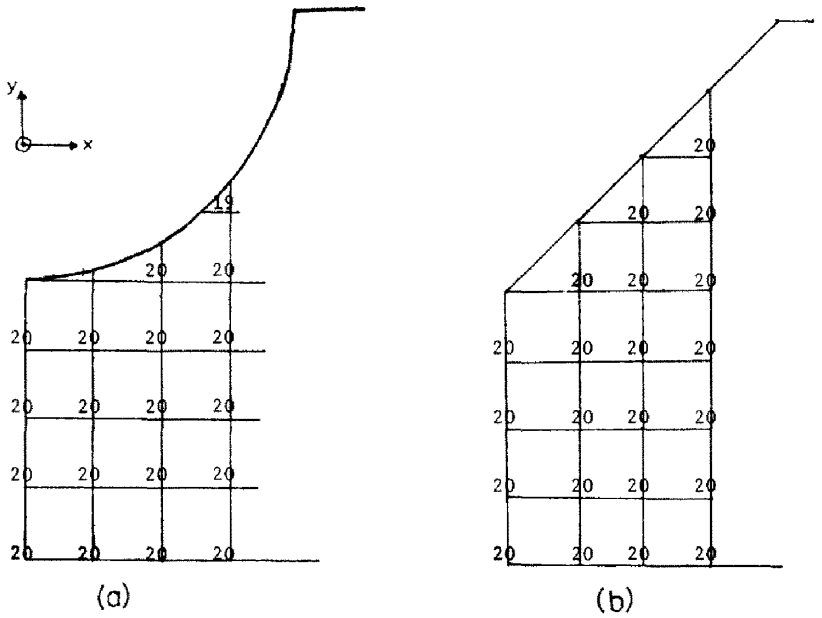

FIG. 6. Generated values of $10p_{xx}$ for $\chi = y^2$.

Obvious modifications in the values assigned to y' must be made at the rounded off corners. On inserting χ, χ' into (1), (2) and solving numerically for σ and μ, we generate stress components in good agreement with those of Southwell and Allen [4]. Contours of constant S and H are exhibited in Figs. 7, 8 and follow broadly the pattern expected.

The extensional problem for V-shaped notches [Fig. 9(a)] may be solved on similar lines. We choose $n = 60$ initially and smooth out the various corners as shown in Fig. 9(b).

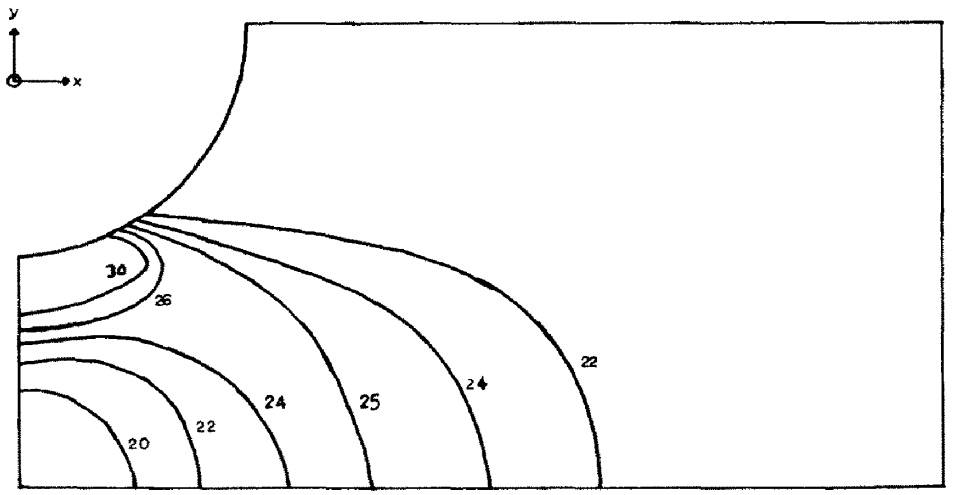

FIG. 7. Extensional problem for a semi-circular notched bar: contours of constant maximum shear stress.

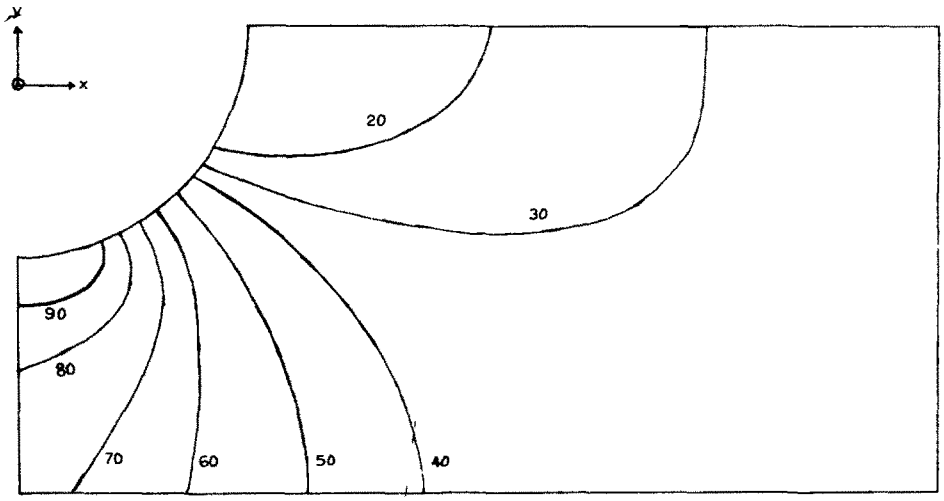

FIG. 8. Extensional problem for a semi-circular notched bar: contours of constant hydrostatic tension.

The second and final subdivision appears in Fig. 9(c). As before, $\chi = y^2$ has been chosen as a test function, and yields the satisfactory generated stress components exhibited in Fig. 6(b). As regards the actual problem, we utilize (34) and (35) except that y' is different along the notch. The generated stress components are seen to compare well with those of Southwell and Allen and contours of constant S and H follow broadly the pattern expected [12].

For problems of uniform bending, the relevant test function is

$$\chi = y^3 \equiv r^2 \cdot \tfrac{3}{4}y + (y^3 - 3x^2y)/4. \tag{36}$$

This enables an encouraging comparison to be made of harmonic and biharmonic sources for the domains exhibited in Fig. 5 and Fig. 9. As regards the actual problem, we have

$\chi_x = 0$ everywhere on L since $F_y = 0$ everywhere on L,

$\chi_y = y^2/2$ on AB taking $F_x = y$ on AB,

$= \frac{1}{2}(\frac{1}{2})^2$ on BCF since $F_x = 0$ on BCF, bearing in mind that χ_y remains continuous at B.

Hence, with obvious modifications in y' at the rounded off corners,

$$\begin{aligned}
\chi' &= \chi_y y' \\
&= 0 \text{ on AB since } y' = 0 \text{ on AB}, \\
&= -\tfrac{1}{8} \text{ on BC since } y' = -1 \text{ on BC}, \\
&= y'/8 \text{ along the notch}, \\
\chi &= \int \chi_y \, dy \\
&= y^3/6 \text{ on AB, choosing } \chi = 0 \text{ when } y = 0, \\
&= \tfrac{1}{6}(\tfrac{1}{2})^3 \text{ on BC since } dy = 0 \text{ on BC} \\
&= y/8 - \tfrac{1}{24} \text{ along the notch, bearing in mind that } \chi \text{ remains continuous at C.}
\end{aligned}$$

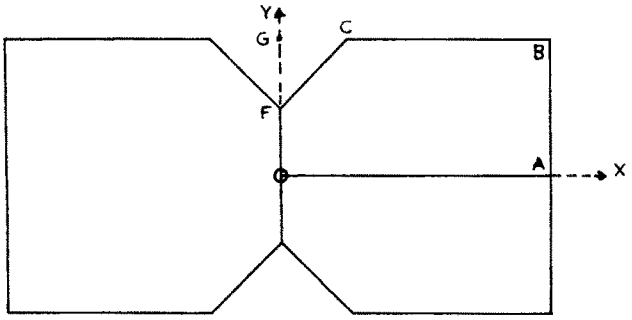

(a) V-shaped notch angle 90° and depth $\frac{1}{4}$.

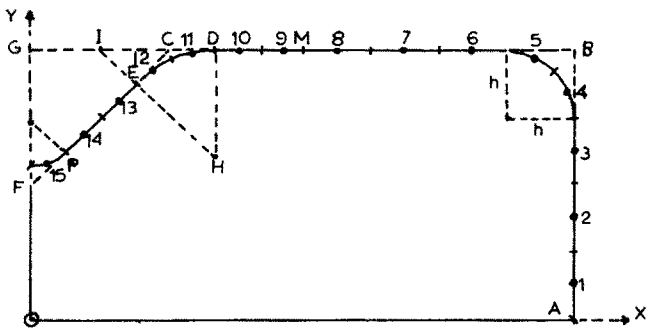

(b) Initial subdivision.

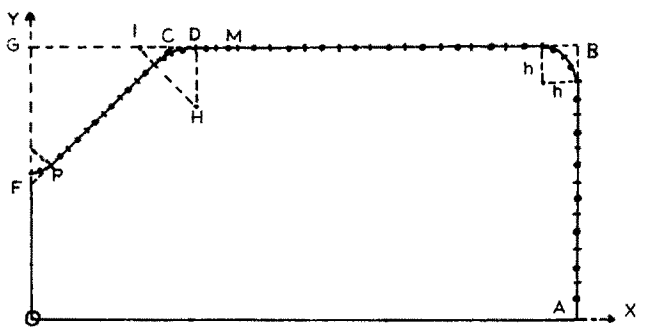

(c) Second and final subdivision.

FIG. 9. To round off the corner at C we construct a circular arc tangential to BC at D and tangential to CF at E. Bearing in mind that $<FCG = 45°$, we have $DH = DI = DC + CI = CE + CE\sqrt{2} = CE(1+\sqrt{2})$. Also $CE = \frac{1}{4}CF$ in (b) and $= \frac{1}{8}CF$ in (c). Note that CD = CE, thereby defining D. Choosing M so that $CM = 2h$, we divide DM into two equal intervals. This enables BM to be divided into the same interval lengths as along AB. The 90° corner at F is rounded off to be a circular quadrant as previously, where PF = CE.

On inserting χ, χ' into (1), (2) and solving numerically for σ and μ, we generate the contours exhibited in Figs. 10 and 11 for a V-shaped notch. Somewhat similar contours are generated for the semi-circular notch. No other solutions seem to be available for comparison.

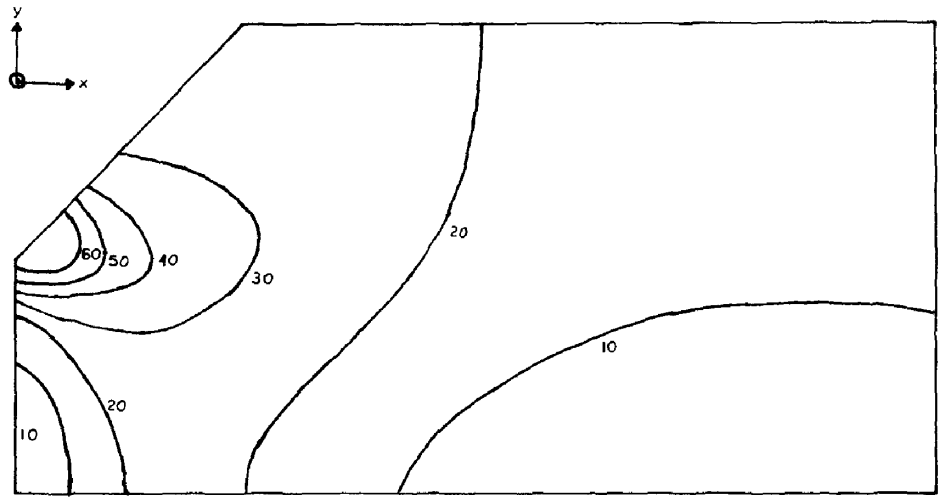

FIG. 10. Bending problem in a V-shaped notched bar: contours of constant maximum shear stress.

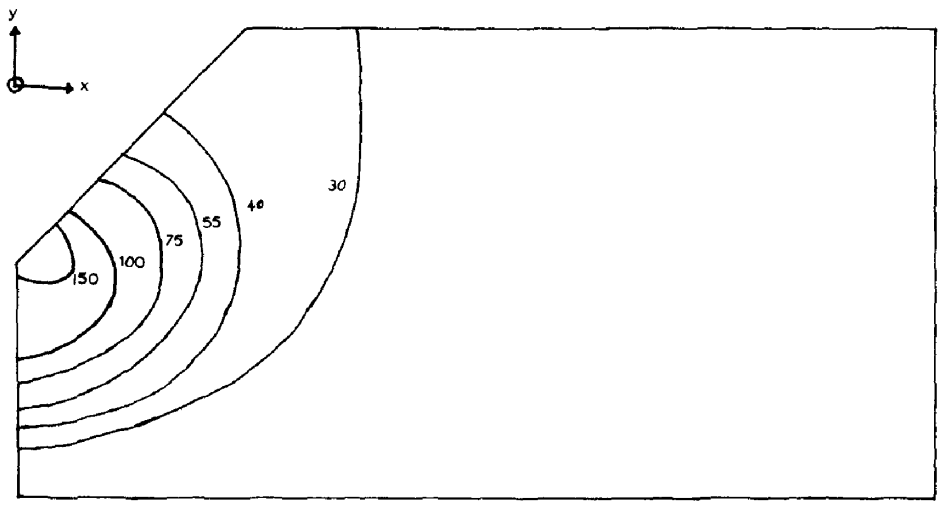

FIG. 11. Bending problem in a V-shaped notched bar: contours of constant hydrostatic tension.

We now consider a semi-infinite medium indented by a rectangular trench of base length $2a$ and depth b, the base being subject to a uniform normal pressure which decreases linearly to zero along the sides (Fig. 12). This problem is of some interest in the field of soil mechanics, but no analytical or numerical solution seems to be available. Evidently the same resultant force operates as previously, and we therefore reflect the problem into the x-axis, separating the domains $y > 0$, $y < 0$ by a cut of finite width to produce the cavity exhibited in Fig. 13(a). As before, all four quadrants are equivalent. Four sections must

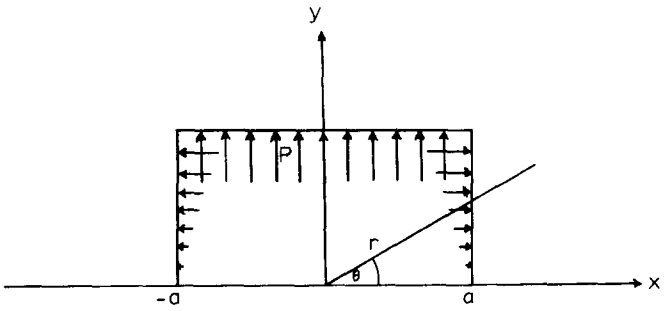

FIG. 12

now be distinguished along L, designated as follows:

1: $0 \leq x \leq a$, $y = b+d$ for which $F_x = 0$, $F_y = P$.

2: $x = a$, $d \leq y \leq b+d$ for which $F_x = P(y-d)/b$, $F_y = 0$,

3: $a \leq x \leq X$, $y = d$ for which $F_x = F_y = 0$,

4: circular extremity, for which $F_x = F_y = 0$.

Hence, along these sections, we have (apart from slight modifications at the rounded off corners)

1: $\chi_x = -Px$, $\chi_y = -Pb/2$,

2: $\chi_x = -Pa$, $\chi_y = -P(y-d)/2b$ since $\mathrm{d}s = -\mathrm{d}y$,

3: $\chi_x = -Pa$, $\chi_y = 0$,

4: $\chi_x = -Pa$, $\chi_y = 0$.

bearing in mind continuity and choosing the constants of integration so that $\chi_x = 0$ when $x = 0$, $\chi_y = 0$ when $y = 0$. Accordingly, we obtain

1: $\chi = -P(x^2+a^2)/2 - Pb^2/6$, bearing in mind $\mathrm{d}y = 0$,

2: $\chi = -P(y-d)^3/6b - Pa^2$, bearing in mind $\mathrm{d}x = 0$,

3: $\chi = -Pax$,

4: $\chi = -Pax$,

bearing in mind continuity and choosing the constant of integration to match (30) as far as possible. χ' presents no difficulty since χ_x, χ_y are known. The problem so formulated has been solved numerically for subdivision $n = 64$ exhibited in Fig. 13(b), and also for $n = 128$, with good conditioning, and yields contours of constant S drawn in Fig. 14 for the cases $b = 0{\cdot}4$, 2. As a check on the reliability of our procedures, we have generated the test function

$$\chi = \cos 2\theta + \log r \equiv r^2 \frac{\cos 2\theta}{r^2} + \log r \tag{37}$$

from the appropriate values of χ, χ' on L. This function is symmetric about both axes,

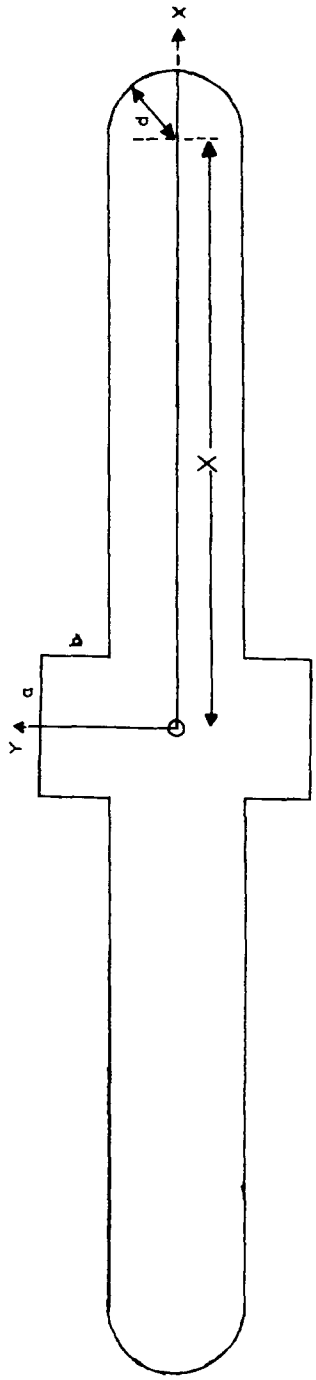

(a) An internal boundary corresponding to Fig. 12.

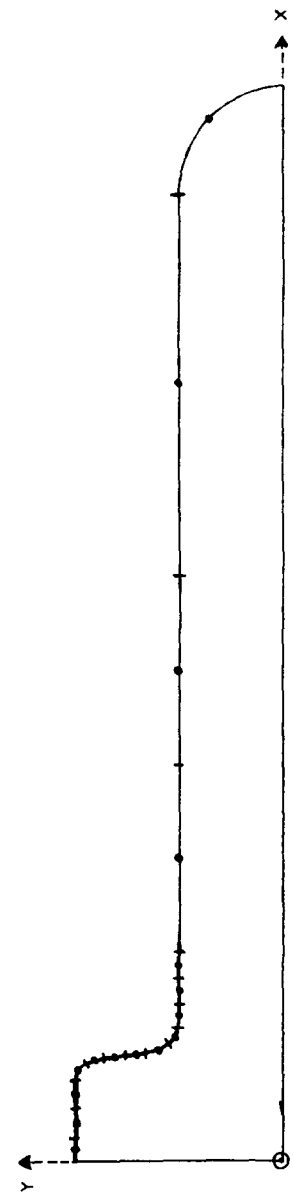

(b) Smoothing and initial subdivision of a quadrant of (a).

FIG. 13

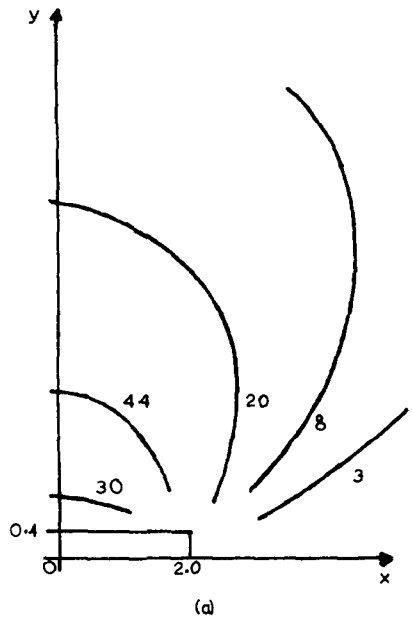

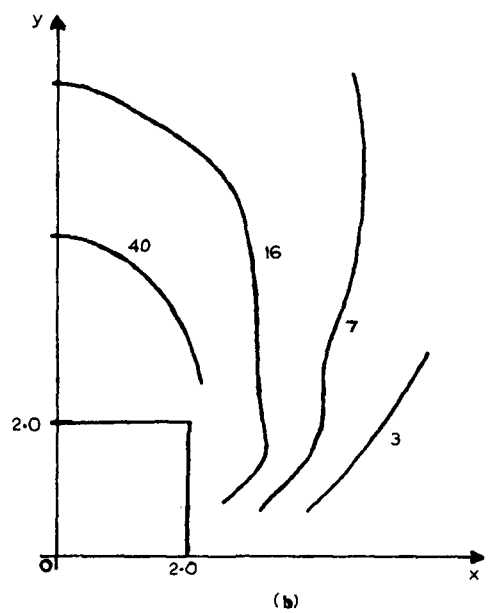

FIG. 14. Contours of constant 400 S^2 for trench of dimensions (a) 4:0·4, (b) 4:2.

and otherwise resembles the above χ in its behavior at infinity. Utilizing the above subdivisions, for the case $b = 2$, we get excellent agreement between the analytical and numerically determined values of S as shown in Fig. 15 for a representative selection of points.

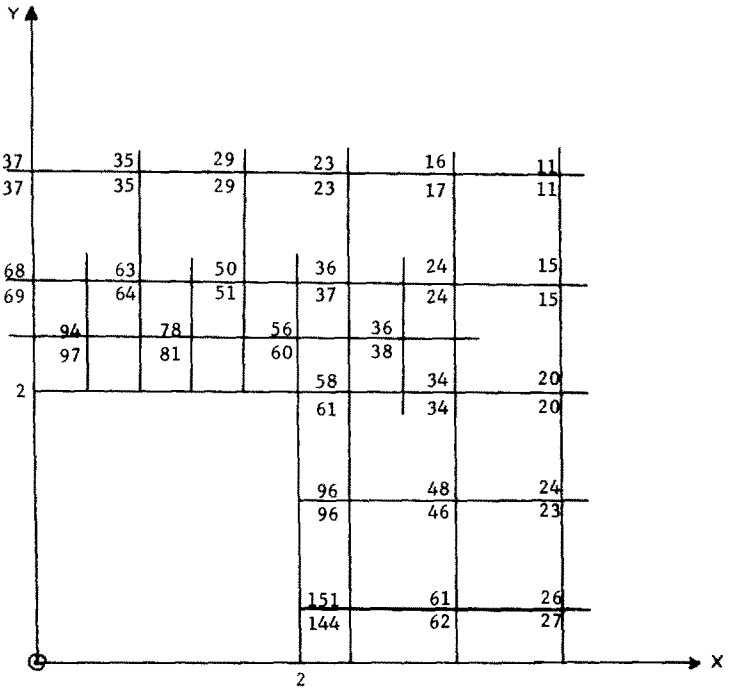

FIG. 15. Generated values of 4000 S^2 (lower) compared with its analytic values (upper) for the test function.

Acknowledgements—Thanks are due to the Director and Staff of the London University Computing Unit for their co-operation. The work of one author (G.T.S.) was carried out as part of a research program at the National Physical Laboratory, England.

REFERENCES

[1] M. A. JASWON, *Proc. R. Soc.* **A 275**, 23 (1963).
[2] G. T. SYMM, *Proc. R. Soc.* **A 275**, 33 (1963).
[3] G. T. SYMM, Ph.D. Thesis, London University (1964).
[4] R. V. SOUTHWELL and D. N. DEG. ALLEN, *Phil. Trans. R. Soc.* **A 242**, 379 (1950).
[5] N. I. MUSKHELISHVILI, *Some Basic Problems of Mathematical Theory of Elasticity*. Noordhoff (1963).
[6] G. T. SYMM, An integral equation method in conformal mapping. *Num. Math.* **9**, 250 (1966).
[7] J. L. SYNGE, *The Hypercircle Method in Mathematical Physics*. Cambridge University Press (1957).
[8] S. BERGMAN and M. SHIFFER, *Kernel Functions and Elliptic Differential Equations in Mathematical Physics*. Academic Press (1953).
[9] F. W. NIEDENFUHR and L. HULBERT, *J. Engng Ind.*, ASME paper No. 64-WA/MD-15.
[10] D. N. DEG. ALLEN, *Relaxation Methods*. McGraw-Hill (1954).
[11] O. D. KELLOG, *Foundations of Potential Theory*. Springer (1929).
[12] M. MAITI, Ph.D. Thesis, London University (1965).
[13] M. A. JASWON and A. R. S. PONTER, *Proc. R. Soc.* **A 273**, 237 (1963).
[14] A. E. H. LOVE, *The Mathematical Theory of Elasticity*, 4th edition. Cambridge University Press (1927).
[15] S. TIMOSHENKO and J. N. GOODIER, *Theory of Elasticity*, 2nd edition. McGraw-Hill (1951).
[16] M. M. FROCHT, *Photoelasticity*, Vol. 1. John Wiley (1941).

APPENDIX I

Given $\chi = r^2\phi + \psi$, the transformation $\phi \to \phi + h(\nabla^2 h = 0)$ implies the compensating transformation $\psi \to \psi - r^2 h$, which requires

$$\nabla^2(r^2 h) = 4\left(x\frac{\partial h}{\partial x} + y\frac{\partial h}{\partial y} + h\right) = 0. \tag{38}$$

Putting $h = S_n$, where S_n is a plane harmonic function of degree n, we see that

$$x\frac{\partial h}{\partial x} + y\frac{\partial h}{\partial y} + h = nS_n + S_n = (n+1)S_n = 0 \tag{39}$$

only if $n = -1$, i.e. $h = r^{-1}\cos\theta$ or $r^{-1}\sin\theta$. These would not be admissible in D_i (provided the origin is located within D_i). They would of course be admissible in D_e. Nevertheless, since

$$\psi = r^2 h = r\cos\theta, r\sin\theta$$

could not be embraced by (16), this transformation would not be admissible for the exterior formulation either. As regards $\chi = x\phi + \psi$ it can be seen directly, or by an application of the above argument, that $\phi \to \phi + c + wy$ may be compensated by $\psi \to \psi - cx - wxy$.

APPENDIX II

To effect a numerical approximation for the integrals in (7) and (8), we divide L into n intervals, the *m-th* interval (of length $2h_m$) being centered about a nodal point $\mathbf{q}_m$ halfway between the interval points $\mathbf{q}_{m\pm 1/2}$. Our fundamental approximation is that $\sigma(\mathbf{q})$ remains constant within each interval, whence we may write

$$\int \log|\mathbf{p}-\mathbf{q}|\sigma(\mathbf{q})\,dq = \sum_1^n \sigma_m \int_m \log|\mathbf{p}-\mathbf{q}|\,dq\,;\ \mathbf{p} = \mathbf{q}_1, \mathbf{q}_2, \ldots \mathbf{q}_n$$

$$\int \log'|\mathbf{p}-\mathbf{q}|\sigma(\mathbf{q})\,dq = \sum_1^n \sigma_m \int_m \log'|\mathbf{p}-\mathbf{q}|\,dq\,;\ \mathbf{p} = \mathbf{q}_1, \mathbf{q}_2, \ldots \mathbf{q}_n$$

where

$$\sigma_m = \sigma(\mathbf{q}_m), \int_m = \int_{\mathbf{q}_{m-1/2}}^{\mathbf{q}_{m+1/2}}$$

Two distinct possibilities arise for $\mathbf{p}$: it may lie outside the m-th interval, which gives no trouble with either integral [2], or it may coincide with $\mathbf{q}_m$, in which case $\int_m \log|\mathbf{q}_m - \mathbf{q}|\,dq$ gives no trouble [2]. Regarding $\int_m \log'|\mathbf{p}-\mathbf{q}|\,dq$, we note [1] that

$$\int_m \log|\mathbf{q}_m - \mathbf{q}|'\,dq + \int^* \log|\mathbf{q}_m - \mathbf{q}|'\,dq = -\pi$$

where $\int^*$ indicates omission of the m-th interval. If so, replacing the m-th interval by a circular arc of radius a, it follows that

$$\int_m \log'|\mathbf{q}_m - \mathbf{q}|\,dq = \int_m \log|\mathbf{q}_m - \mathbf{q}|'\,dq = -\pi - \int^* \log|\mathbf{q}_m - \mathbf{q}|'\,dq \tag{40}$$

since

$$\log'|\mathbf{q}_m - \mathbf{q}| = \log|\mathbf{q}_m - \mathbf{q}|' = -1/2a \tag{41}$$

for such an arc. Evaluation by (40) ensures that the discrete system which replaces equation (8), considered as an integral equation for σ, has a singular matrix, as is required. However, in so far as (8) forms part of the biharmonic formulation (1) and (2), it would suffice to write

$$\int_m \log'|\mathbf{q}_m - \mathbf{q}|\, dq = -2h_m/2a = -h_m/a \tag{42}$$

by virtue of (41). Accordingly, whereas (40) has been used by Symm, (42) has been used in the present paper.

(*Received* 11 *April* 1966; *revised* 12 *September* 1966)

Résumé—Il est démontré que des problèmes de valeur de limite biharmonique peuvent être formulés en termes d'équations intégrales. Des procédés sont donnés pour résoudre ces équations numériquement, pour adoucir les angles aigus des limites et pour vérifier les résultats. Ces techniques sont appliquées pour attaquer quelques problèmes de tension à deux dimensions qui ne semblent pas être favorables à aucun autre traîtement.

Zusammenfassung—Es wird gezeigt, dass biharmonische Grenzwertsprobleme als Integralgleichungen ausgedrückt werden können. Vorgänge für die Lösung dieser Gleichungen werden gegeben, sowohl für die numerische Lösung wie auch für die Rundung scharfer Ecken der Grenzen, ferner auch für die Prüfung der Resultate. Diese Methoden werden auch zur Lösung zweidimensionaler Spannungsprobleme gebraucht, die sonst keine Lösung haben.

Абстракт—Показано, что проблемы бигармонического граничного значения могут быть сформулированы с точки зрения интегральных уравнений. Даются методики проведения решения таких уравнений численно, для сглаживания резких углов на краю и для проверки результатов. Эти технические методы применяются для подхода к решению некоторых проблем двумерного напряжения, которые, повидимому, не поддаются никакому другому обращению.